Fine Structure of Singly Ionized Helium*

EDGAR LIPWORTH† AND ROBERT NOVICK‡
Columbia Radiation Laboratory, Columbia University, New York, New York
(Received August 10, 1956)

The separation in energy (S) between the $2\,^2S_{\frac{1}{2}}$ and $2\,^2P_{\frac{1}{2}}$ states of singly ionized helium has been measured to high precision by a microwave method. Helium atoms in a resonant cavity are excited to the $2\,^2S_{\frac{1}{2}}$ state of the ion by bombardment with 300-volt electrons. Rf power is applied to induce transitions between the two states and the 40.8-ev photon which arises from the decay of the $2\,^2P_{\frac{1}{2}}$ state to the $1\,^2S_{\frac{1}{2}}$ ground state of the ion is detected by a photomultiplier tube. A method of synchronous detection is employed to improve the signal-to-noise ratio. Twenty-six determinations of (S) have been made under differing experimental conditions in an attempt to uncover sources of systematic error.

The value of (S) obtained for He^+ is $14\,040.2\pm4.5$ Mc/sec. The uncertainty is equal to three times the standard deviation plus an estimated 1.5 Mc/sec for the uncertainty in various systematic corrections. The result is in agreement with previous determinations but differs significantly from the best available theoretical value of $14\,056.8\pm3.0$ Mc/sec. It is shown that this discrepancy might be resolved, without impairing the excellent arrangement in hydrogen, by a theoretical relativistic term of the form $\alpha(\alpha Z)^6 \ln(\alpha Z)$.

INTRODUCTION

THE fine structure of the $n=2$ state of hydrogen has, over the past few years, been subjected to a very detailed examination by Lamb and his collaborators.[1] This work has established that a small separation exists between the $2S_{\frac{1}{2}}$ and $2P_{\frac{1}{2}}$ levels of the atom that has its origin in the interaction of the electron with the quantized vacuum radiation field. The theoretical value of this radiative shift is obtained from quantum electrodynamics as a series in the quantity (αZ) where α is the fine structure constant and Z is the nuclear charge; only a few of the lower order terms have been evaluated so far. The value of the shift obtained from these terms is in excellent agreement with the measurements in hydrogen. A precise measurement of the shift in singly ionized helium will indicate the relative importance of the higher order terms.

The first measurement upon singly ionized helium was made by Skinner,[2] but her work was of an exploratory nature and not intended for precise measurement. In 1950 a program was initiated to determine the level shift (S) to a precision that would bear comparison with that of the hydrogen experiments. The first results were obtained by Novick *et al.*, who measured $(S)=(14\,043\pm13$ Mc/sec$)^2$. This measurement was made using an elaborate pulse method due to Yergin[3]; the equipment was complex and cumbersome and the work was plagued by vacuum contamination effects, both factors contributing to prevent the accumulation of sufficient data for the study of systematic sources of error.

In the present work a considerable simplification has been achieved by the use of a synchronous, or lock-in, detection scheme in place of the pulse method referred to above. Great precautions have been taken to eliminate the instabilities due to vacuum contamination, with the result that a large body of data has been accumulated under different conditions. The transition studied has π polarization and therefore a different magnetic field dependence than the σ transition observed by Novick. Perhaps more important is the fact that space-charge conditions within the interaction region are completely different from those occurring in the earlier work, with the effect that the corrections that must be applied to the results have been evaluated from a different standpoint.

I. METHOD

Helium gas in a resonant microwave cavity is bombarded continuously with 300-ev electrons and a small fraction of the bombarded helium atoms is ionized and excited to the $2\,^2S_{\frac{1}{2}}$ metastable state of interest.[4] An externally applied magnetic field splits the $2\,^2S_{\frac{1}{2}}$ and neighboring $2\,^2P_{\frac{1}{2}}$ levels as shown in Fig. 1. When rf power of the correct frequency is fed into the cavity, an electric dipole transition is induced between the levels labeled α and e. Ions that are transferred from the state α to the state e decay very rapidly ($\tau=10^{-10}$ sec) to the $1\,^2S_{\frac{1}{2}}$ ground state, each emitting a 40.8-ev photon. Some of the photons escape through a grid in the wall of the cavity and fall upon the photocathode

* Work supported jointly by the Signal Corps, the Office of Naval Research, the Air Research and Development Command, and the National Science Foundation.

† Present address: Radiation Laboratory, University of California, Berkeley, California.

‡ Present address: Department of Physics, University of Illinois, Urbana, Illinois.

[1] The series of papers on the hydrogen experiments will be referred to as HI, HII, HIII, HIV, HV, HVI. These are: HI—W. E. Lamb, Jr. and R. C. Retherford, Phys. Rev. **79**, 549 (1950); HII—W. E. Lamb, Jr. and R. C. Retherford, Phys. Rev. **81**, 222 (1951); HIII—W. E. Lamb, Jr., Phys. Rev. **85**, 259 (1952); HIV—W. E. Lamb, Jr. and R. C. Retherford, Phys. Rev. **86**, 1014 (1952); HV—Triebwasser, Dayhoff, and Lamb, Phys. Rev. **89**, 98 (1953); HVI—Dayhoff, Triebwasser, and Lamb, Phys. Rev. **89**, 106 (1953).

[2] The series of papers on singly ionized helium will be referred to as HeI, HeII. These are: HeI—W. E. Lamb, Jr. and M. S. Skinner, Phys. Rev. **78**, 539 (1950); HeII—Novick, Lipworth, and Yergin, Phys. Rev. **100**, 1153 (1955).

[3] P. F. Yergin, thesis, Columbia University, 1953 (unpublished).

[4] See Fig. 2 of HeII.

of an Allen-type[5] photomultiplier tube and the resulting photoelectric current pulse is amplified and counted.

In the absence of rf power, about 1% of the ion content of the cavity is in the metastable state; the remainder consists of ions in the ground state or in other excited states. The rf-induced signal forms a small addition to a large background arising from the decay of excited short-lived states of the atom and ion. The microwave cavity is designed so that the electric vector of the rf field is parallel to the applied magnetic field; αe is a π transition. The radio-frequency is chosen so that the αe resonance peak occurs at a magnetic field close to that necessary to cause levels β and f to cross each other. The reasons for this choice are set forth in Sec. VIID.

In order to make clear the reasons for the measurement procedure adopted, it is instructive to consider the difficulties which might be encountered if one tried to measure the resonant frequency simply by determining the counting rate as a function of magnetic field. First, the rf-induced signal is a small fraction of the background signal, about 1/20 in a typical instance at the resonance peak. This would not itself be objectionable if the background signal were stable, but changes in counting efficiency which derive from changes in the gain of the Allen tube and its associated amplifiers cause the background signal to fluctuate by several percent during the course of a run. Second, the background signal itself contains a component which is field dependent, the so-called β-state signal arising from metastable ions in the $2\,^2S_{\frac{1}{2}}(m_s=-\frac{1}{2})$ state which are strongly coupled to the $2\,^2P_{\frac{1}{2}}(m_s=-\frac{1}{2})$ state by the longitudinal space-charge electric field. Since the resonance is observed by varying the magnetic field, the β-state signal is magnetic-field-dependent and the resulting field dependence of the background might produce a shift in the resonance center.

Some means, therefore, is required to eliminate or reduce the effect of the foregoing factors. The procedure adopted is to modulate with a square wave the rf power at a 500-cps rate. The signal from the Allen tube is fed to two scalers connected in parallel; when the rf power is "on" Scaler I is gated to count and Scaler II is gated off. When the rf power is "off" the reverse situation obtains. Scaler II therefore provides a measure of the background signal close in time to the rf-induced signal. The background signal does not change appreciably in 1/500 sec so that the quantity ϕ, called the normalized rf signal and defined by

$$\phi=[(N_{\mathrm{I}}-N_{\mathrm{II}})/N_{\mathrm{II}}]\times 100, \tag{1}$$

is a measure of the rf-induced signal normalized to unit background. N_{I} and N_{II} are the counts in Scalers I and II, respectively. At each field two quantities, ϕ_L and ϕ_H are measured. ϕ_H is the normalized rf signal observed with sufficient power to quench all the metastable ions exposed to the detector as soon as they are formed. ϕ_L is the corresponding quantity at a power level sufficient to quench only 30% or so of the total metastable population, at the resonance center.

The quantity,

$$\psi=(\phi_L/\phi_H)\times 100, \tag{2}$$

called the percentage rf quenching, when plotted as a function of magnetic field defines the resonance. Since the main contribution to the background signal arises from the excitation and decay of short-lived states of the ion, and both the background and rf-induced signals produce single photoelectrons at the Allen tube photocathode, the pulse-height distribution of the two signals is the same. Hence the above described normalization procedure effectively compensates for changes in the detection efficiency. If the assumption is made that the fractional contribution of the β-state signal to the background is the same for ϕ_L and ϕ_H, then ψ is independent of variations in the β-state signal. It should be noted that ϕ_H is a measure of the rate of production of metastable ions normalized to unity background, and that implicit in the above discussion is the assumption that this rate together with the rate of production of ground state ions, is field-independent. Since the path length of the exciting electrons within the cavity is independent of the magnetic field, and since there are strong reasons for regarding the ion production cross sections as, for all practical purposes, field-independent also, it is felt that the normalization procedure has validity. However, resonance distortions produced by changes in the ion removal rate due to changes in the space-charge electric fields when the magnetic field is varied are not compensated by the normalization procedure. This matter will be taken up again in Sec. VIIG.

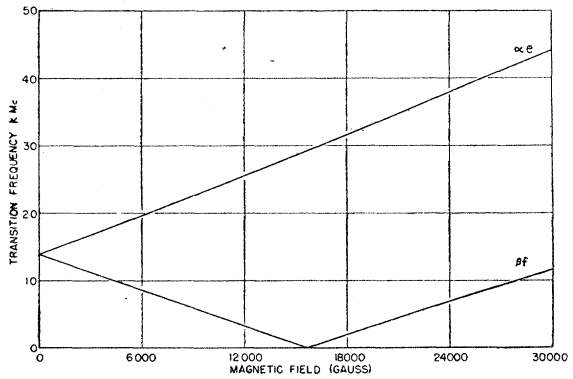

FIG. 1. Transition frequency *versus* magnetic field for the $\Delta m=0$ transitions between the $2^2S_{\frac{1}{2}}$ and $2^2P_{\frac{1}{2}}$ states in He^+. The α, β, e, f notation is defined in Fig. 3 of HeII.

[5] J. S. Allen, Rev. Sci. Instr. 18, 739 (1947).

II. APPARATUS

A cross section of the apparatus is similar to that shown in Fig. 5 of HeII. The essential parts are (1) an interaction cavity containing helium gas, situated between the poles of an electromagnet, (2) an Allen-type

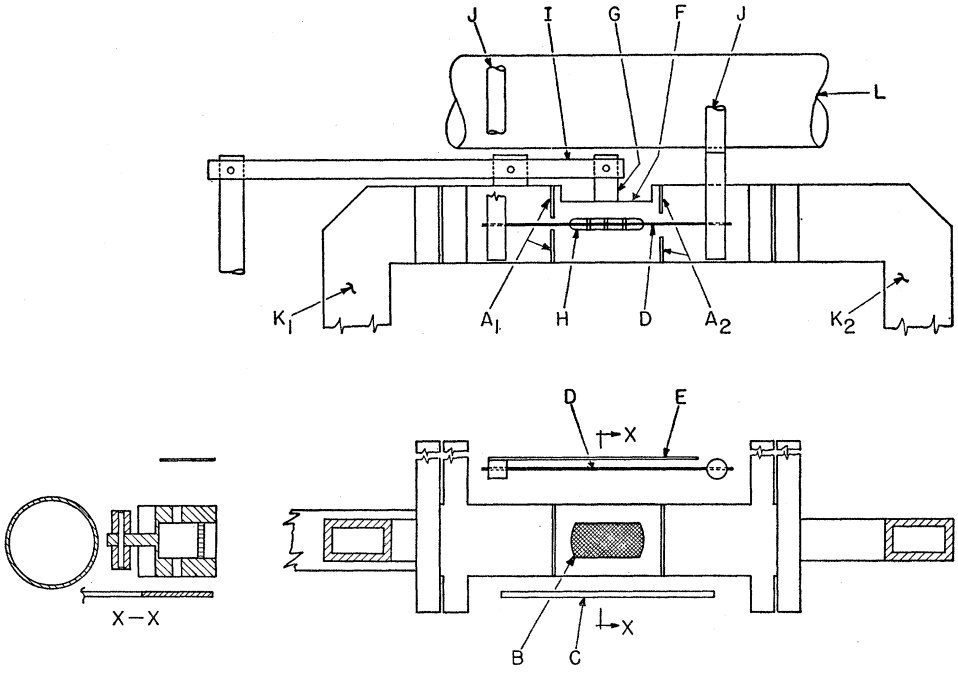

FIG. 2. Cross section of interaction space and electron gun structure. $A1A2$—Irises; B—photon exit grid; C—electron collector plate; D—filament; E—filament shield; F—0.005-in. wall; G—tuning stub; H—electron beam entrance slot; I—mechanical tuner; J—filament support posts; $K1,K2$—wave guide; L—nuclear magnetic resonance detector probe.

photomultiplier detector that connects with the interaction cavity through a platinum light pipe, (3) a thin Formvar film across the pipe to prevent helium entering the photomultiplier, and (4) a nuclear absorption magnetometer probe near the cavity to measure the magnetic field. Since the apparatus differs in many important ways from that described in HeII, a brief description of it will be given.

A. Vacuum System

In order to avoid the troublesome contamination effects noted in the introduction, a vacuum system has been constructed for the present experiment which incorporates a minimum of organic material. All seals are made with Teflon O rings and the system pumped with mercury pumps. A Freon-cooled baffle and liquid-nitrogen trap after each pump prevents mercury from distilling up into the interaction region and Allen tube housing. A Freon-cooled trap behind each pump prevents mercury from depositing in the rotary pumps and minimizes possible contamination of the system by oil vapors from the latter. The main liquid-nitrogen traps hold a charge of nitrogen for 24 hours and the system, once evacuated, was run continuously between disassemblies. The entire vacuum system, apart from the interaction envelope, was made from steel, nickel plated for reasons of cleanliness. The interaction envelope was constructed from O.F.H.C. copper. Because of the high magnetic field required (15 600 gauss), it was important to maintain as small a pole-piece gap as possible. The pole-piece tips were soldered into the envelope and formed part of the upper and lower vacuum wall. The interior of the envelope was gold-plated.

B. Interaction Space

The interaction space is shown in Fig. 2. The cavity was hobbed from a solid piece of O.F.H.C. copper, the resonant section being defined by irises A_1A_2 set into the side walls. The dimensions are such that at the frequency employed the cavity proper forms a section of waveguide that is within 6% of cutoff. The back face of the cavity was cut down to leave a wall F, 0.005 in. thick, carrying a projection G; small deformations of this back wall via the lever I could be produced by a differential screw outside of the vacuum wall. The cavity could thus be tuned over a small range of frequency (approx 0.14%).

The electron beam entrance and exit slots H were reticulated with thin copper slats to reduce microwave radiation loss. A Sperry honeycomb klystron grid B, set into the front wall, served as an exit port for the signal photons. The grid slats and the photon grid were soldered into place in a hydrogen furnace with BT solder (melting point 778°C) and the whole cavity could be cleaned by heating to a dull red heat in a hydrogen atmosphere.

The cavity is supported on one vacuum face plate by waveguide sections K_1K_2. Power is fed into the cavity via K_1 and the power coupled to K_2 through the irises A_2 serves as a measure of the power level inside the cavity.

The electron gun assembly, consisting of a filament D, collector C, and shield E, is mounted on a second face plate that closes the opposite end of the vacuum envelope. Extreme care had to be exercised during manufacture of the electron gun and collector assembly on the one hand, and the interaction space and wave-

guide assembly on the other, in order that the two be properly aligned with respect to each other when mounted. The filament is maintained at a potential of -300 v with respect to the cavity and heated with approximately 6 amperes of 100-kc rf current to prevent its displacement in the static magnetic field. The shield E at filament potential prevents electron bombardment of the vacuum wall. The electron collector plate C is held 45 v positive with respect to the cavity, and low-energy secondaries are thereby prevented from entering the interaction region.

C. Detector and Counting System

Apart from minor modifications, the counting system is identical with that described in HeII.

D. Magnetic Field

The magnet current is regulated by the same regulator used by Lamb and Retherford in the hydrogen experiment, modified for use at the higher fields now employed. The total magnet current of approximately 8 amperes is passed through thirty 6336 vacuum tubes[6] connected in parallel, and the control voltage applied to the grids of these tubes. This device holds magnet field current steady to about one part in 100 000 for short periods of time.

The magnetic field is measured with a proton-resonance absorption apparatus designed to operate at high frequencies. The oscillator covers a frequency range of 54 to 86 Mc/sec or 12 400 to 18 800 gauss. Because of the high frequencies involved, the sample coil is coupled to the oscillator by a length of cable approximately $\frac{1}{2}\lambda$ in length. As the frequency is varied, the length of the line is adjusted to maintain approximately the line length of $\frac{1}{2}\lambda$ by switching in additional lengths of cable with two coaxial switches. Six steps are required to cover the range 54 to 80 Mc/sec.

The magnetic fields that can be set up at the probe are restricted to values that correspond to 100-kc steps in the proton resonance frequency. 100-kc markers derived from a frequency standard are arranged to cover the working spectrum of the oscillator, which is beaten with a selected one of the markers. Identification of the appropriate marker is made with the help of a General Radio type 620-A heterodyne frequency meter. The center of the nuclear magnetic resonance probe is situated 1.65 cm from the center of the interaction region. At the high fields employed, the field at the probe is nonuniform and as a consequence the proton resonance is broad, with widths of 4.2 and 6.3 gauss at the low- and high-field working points, respectively, and it is only possible to set up a particular field at the probe to about ± 1 gauss.

The difference between the values of the field at the probe and at the center of the cavity is appreciable, six

[6] Supplied by Chatham Electronics Corporation, Livingston, New Jersey.

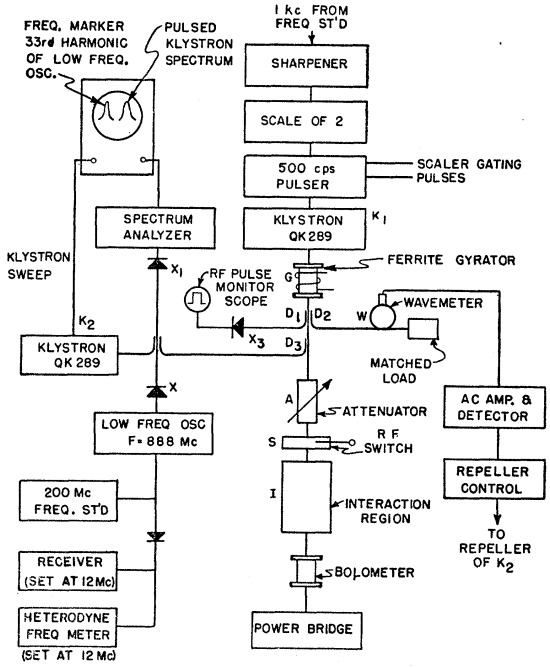

FIG. 3. Radio frequency apparatus. The connection from the repeller control is incorrect, it should be connected to K_1 rather than K_2. The frequency standard is incorrectly labelled; it should be 100 Mc/sec.

gauss at the low field working point and ten gauss at the high. A sizeable inhomogeneity correction is therefore required, which was measured by replacing the cavity with a magnetometer whose sample geometry conformed as closely as possible to that of the ion beam. The magnet was cycled through zero field several times to establish that the inhomogeneity correction remained constant.

E. Radio-Frequency Equipment

The rf system is shown in Fig. 3. A 500-cps square wave is applied to the repeller of a Raytheon QK289 klystron K_1. A ferrite gyrator G serves to isolate the klystron from changes in the load. After passing through the variable attenuator A, and switch S, the power is fed into the interaction region I; the small amount of power coupled through the back irises of the cavity is monitored with a PRD[7] type-617 bolometer in conjunction with a PRD type-277 standing-wave amplifier. A small amount of power is withdrawn from the main guide by directional couplers D_1, D_2, and D_3 to monitor the rf envelope, stabilize[8] the klystron, and measure its frequency. The signal from D_3 is mixed with that from a swept klystron K_2 in crystal X_1. The 40-Mc/sec difference frequency from X_1 is passed into

[7] Polytechnic Research and Development Company, Brooklyn, New York.

[8] The regulator employed is similar to that described by E. S. Dayhoff, Rev. Sci. Instr. 22, 1025 (1951).

a Massachusetts Institute of Technology spectrum analyzer, type TSK-1SE, whose output is presented on an oscilloscope. The scope picture is a pip approximately 0.3 Mc wide at the $\frac{1}{2}$-power point, the width being determined mainly by the IF band width of the spectrum analyzer. The thirty-third harmonic of a low-frequency oscillator is produced in X and the resulting marker presented simultaneously on the oscilloscope with the pip from K_1.

The low-frequency oscillator is held at a constant frequency by comparison with a frequency standard so that when the two markers are superimposed the klystron frequency is 29 304±0.5 Mc/sec, corresponding closely to the αe transition frequency at the βf crossing point. During all runs care was taken to ensure that the klystron frequency was held within the above limits. The repeller electrode of the pulsed klystron is square wave modulated at a 500-cps rate in a way that ensures the positive and negative portions of the square wave are as much the same as possible. The scaler gating pulses are obtained from the same unit that supplies the klystron modulation pulse and are accurately phased with the latter.

At the power level required to record resonance data, the emergent power from the cavity is about 1 microwatt, which is too small an amount to measure accurately on a direct-reading power bridge. The effective sensitivity of the bolometer was increased considerably by making use of the fact that the rf is modulated. The bolometer output is fed into the PRD type-277 amplifier mentioned above and the rectified output presented directly on a meter. The ultimate sensitivity of such a system with a PRD type-617 bolometer is approximately 3×10^{-10} watt, which is 3000 times less than the minimum power level employed.

Since it is important that the power level be held constant, the gain of the amplifier was checked frequently. This was accomplished by calibrating it with a 500-cps signal derived from a Stevens Arnold chopper and a mercury cell. The rf power can be held constant to a fraction of a percent.

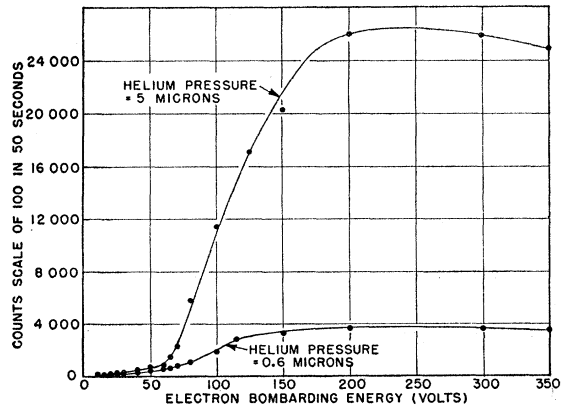

FIG. 4. Helium excitation curves. The signal is proportional to pressure, the fact that it does not appear to be so here is due to a change in Allen tube voltage, and therefore detection efficiency, between observation of the two curves.

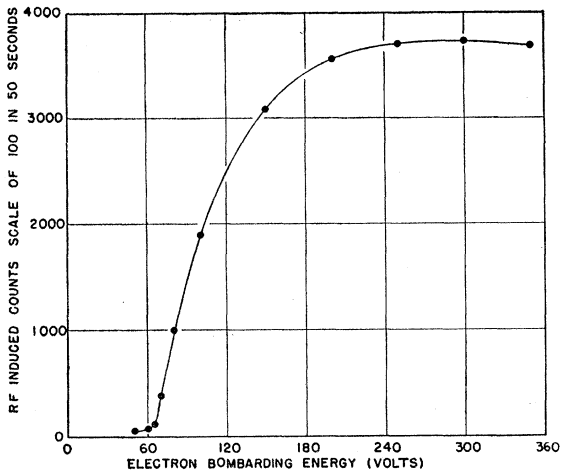

FIG. 5. Rf-induced counts as a function of electron bombarding energy.

III. OPERATING CHARACTERISTICS OF THE APPARATUS

A. Allen Tube Detector

The Allen tube detector is identical with that described in HeII. The background was normally less than 10 counts/min at an applied voltage of 3 kv. Signal counts were approximately 10^7 counts/min.

B. Excitation Curves

Excitation curves of the background and rf-induced signals are shown in Figs. 4 and 5. The two curves of Fig. 4 were observed at two different helium pressures, one approximately ten times the other. The sharp change in signal at 65 volts on the high-pressure curve is due to the onset of excitation of the $2P$ states of the He ion. (The first excited state of He^+ occurs at 65.4 ev relative to the ground state of the atom.) The fact that the excitation curve rises steeply at the point that it does, indicates that the main contribution to the background signal arises from ionic states of He; below 65 volts only atomic states are excited. Since the atomic excitation process is a one-step process rather than a two-step one as in the case of the ion, one would expect to have a larger signal from atomic than ionic states. However, two factors contribute to reduce the former signal:

(1) The long column of helium gas between the cavity and Formvar film serves to scatter resonantly the photons arising from atomic states many times before they can reach the detector. The absorption and re-emission of a photon does not necessarily mean that it is lost to the detector, but it is likely that a photon that strikes the wall of the light pipe several times will be absorbed.

(2) The Formvar film should act as a selective filter for atomic-state photons, since it is known that Formvar has a higher absorption coefficient for 20-ev photons than for 40-ev photons.[9] An important service performed by the film is the prevention of metastable helium atoms from reaching the Allen tube photocathode, where they would give rise to a signal.

The effect of resonance scattering can be seen by comparing the two curves of Fig. 4. At low pressure where the resonant scattering is small, the atomic contribution to the total signal is relatively much larger than in the high pressure case.

As would be expected, the excitation curve for the rf-induced signal exhibits a sharp rise at 65 volts (Fig. 5). The small rf-induced signal below the threshold is due to metastable ions, formed in the region between the cavity and electron collector plate, moving into the rf field. The collector was maintained 45 v positive with respect to ground so that electrons need only be initially accelerated to 20 v to begin to produce metastable ions. In order to maximize the rf-induced signal the bombarding voltage during all runs was chosen to be 300 v.

C. Scaler Dead Time

Counting rates are high and a correction is required due to scaler dead time. A discussion of dead-time losses is deferred to Appendix I.

D. Stability of Data

In the absence of contaminations and other sources of signal instability, one would expect the observed fluctuations in the percentage rf quenching, ψ, to be determined by counting statistics alone. In practice, however, ψ is a function of the following parameters which themselves are subject to fluctuation:

(1) rf power, (Y),
(2) bombarding current, (i),
(3) helium pressure, (p),
(4) klystron frequency, (f_k),
(5) magnetic field, (H).

We have, therefore,

$$\psi=\psi(Y,i,p,f_k,H)=\psi(x_j),$$

and

$$\langle\Delta\psi\rangle_p=\left[\sum_j\left(\frac{\partial\psi(x_j)}{\partial x_j}\right)^2(\Delta x_j)^2\right]^{\frac{1}{2}},\qquad(3)$$

where $\langle\Delta\psi\rangle_p$ is the expected rms deviation in ψ due to fluctuations in the parameters. If $\langle\Delta\psi\rangle_N$ be defined as the expected rms deviation due to the counting statistics alone, then

$$\langle\Delta\psi\rangle_{\text{tot}}=[\langle\Delta\psi\rangle_p{}^2+\langle\Delta\psi\rangle_N{}^2]^{\frac{1}{2}},\qquad(4)$$

where $\langle\Delta\psi\rangle_{\text{tot}}$ is the expected total rms fluctuation in ψ.

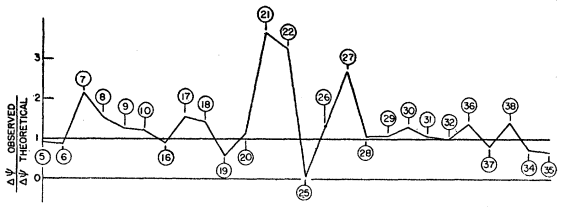

FIG. 6. Observed$\langle\Delta\psi\rangle$/theoretical$\langle\Delta\psi\rangle$ for useful runs.

A study has been made of the dependence of ψ upon the various parameters listed and the results, together with a reasonable estimate of the magnitudes of the Δx_j, have been used to compute a $\langle\Delta\psi\rangle_{\text{tot}}$ for all 25 runs that constitute the main body of experimental data. The results are summarized in Fig. 6 where the ordinate is the ratio of the observed rms fluctuation in ψ to $\langle\Delta\psi\rangle_{\text{tot}}$. A simple statistical test (Snedcor's test) indicates that deviations in the ratio from unity are purely statistical with the exception of runs 7, 21, 22, and 27. The reason for the excess fluctuation in these four runs is not known but may be attributable to surface contamination of the cavity walls, or to a fault in the electronic system.

IV. REMOVAL PROCESSES

In order to discuss the experimental results adequately and obtain measures of the corrections that must be applied to the observed value of the radiative shift (S), it is necessary to have an understanding of the processes that govern the motion of ions within the cavity. It will be shown that the dominant ion removal process is due to the space-charge electric fields within the ion stream. As a preliminary to a discussion of the space-charge-dominated phenomena, less significant removal processes will be treated first. Some of these depend upon a knowledge of the space-charge fields and the results of subsequent sections will be freely employed when necessary.

A. Natural Radiative Decay

Direct transitions between the metastable $2\,{}^2S_{\frac{1}{2}}$ state and the $1S_{\frac{1}{2}}$ ground state of ionized helium are forbidden by the $\Delta l=\pm1$ selection rule. Transitions to the $2P_{\frac{1}{2}}$ states are allowed, but because of the small energy separation, proceed slowly in the absence of an electric field. The most likely decay mechanism for the $2\,{}^2S_{\frac{1}{2}}$ state is believed to be two-quantum decay, for which the lifetime is 2.2×10^{-3} sec.[10]

B. Ion Thermal and Recoil Motions

The helium gas will be assumed to be in equilibrium at a temperature equal to that of the walls of the cavity.

[9] G. L. Weissler and L. Z. Maudlin, Phys. Rev. **100**, 1800(A) (1955).

[10] G. Breit and E. Teller, Astrophys. J. **91**, 215 (1940).

The cavity temperature is raised by its proximity to the filament. The equilibrium temperature has not been presently measured, but it was measured for HeII and found to be 130°C and this value will be assumed here, though it is probably a little high due to better cooling.

Since the ions, when produced, spiral about the magnetic field lines, the thermal velocity appropriate to removal is the average thermal velocity along the field lines. In the present case $v_{\text{thermal}}=0.92\times10^5$ cm/sec. The maximum and minimum recoil velocities are given by the expression[11]

$$v_{\text{recoil}}=\frac{m}{M}\left[\pm v_0+\left(2v_0^2-\frac{4Q}{m}\right)^{\frac{1}{2}}\right], \tag{5}$$

where the + sign is taken for the maximum recoil velocity and the − sign for the minimum. The symbols are defined in reference 11. We have:

$$\begin{aligned} v_{\text{recoil}}(\text{max})&=3.16\times10^5 \text{ cm/sec},\\ v_{\text{recoil}}(\text{min})&=0.34\times10^5 \text{ cm/sec}. \end{aligned} \tag{6}$$

The kinematics upon which Eq. (5) is based are of course not sufficient to determine the distribution of recoil velocities or the average recoil velocity. Mott and Massey, however, have made a calculation of the velocity distribution of electrons ejected in ionizing collisions with hydrogen atoms.[12] They find that the average velocity of the ejected electrons, for 300-ev incident electrons, is about $Z\alpha c$, the mean velocity of an electron in a K shell; α is the fine structure constant and c the velocity of light. In the absence of further information, the average velocity of ejection in the present case will be taken as $Z_{\text{eff}}\alpha c$, where $Z_{\text{eff}}=1.69$, and the average recoil momentum of the resulting ion assumed to be equal to the average linear momentum of the ejected electron.

Thus if M is the mass of the ion and v_{recoil} its average velocity, we have

$$\begin{aligned} v_{\text{recoil}}&=Z_{\text{eff}}\alpha c(m/M)\\ &=0.51\times10^5 \text{ cm/sec}. \end{aligned} \tag{7}$$

In view of the crudeness of this estimate, the average recoil velocity and not its projection along the field lines will be assumed to be the effective velocity. The resultant velocity v_R which in part determines the ion removal time will be taken as $[(0.51)^2+(0.92)^2]^{\frac{1}{2}}=1.05\times10^5$ cm/sec. The speed of spiral motion around the field lines is then $1.05\times\sqrt{2}\times10^5=1.48\times10^5$ cm/sec.

The removal time due to thermal and recoil effects is given by

$$\tau=d/v_R, \tag{8}$$

where d is the height of the *rf* quenching region, $d=0.46$ cm, and $\tau=4.4$ μsec.

C. Stark Quenching

In the presence of an electric field there is a mixing of the $2\,^2S_{\frac{1}{2}}$ state of the ion with the adjacent short-lived $2\,^2P_{\frac{1}{2},\frac{3}{2}}$ states, with a consequent reduction in the lifetime of the former. The decay constant of the mixed state has been evaluated by Lamb and is given by Eq. (76) of HI.

The ions, in their passage through the cavity, are acted upon by space-charge and motional electric fields. An upper bound of 8 volt/cm for the space-charge field under normal operating conditions has been set in Sec. IVF.

The motional field is given by $\mathbf{E}=\mathbf{v}\times\mathbf{H}/c$, where v is the velocity of the ions, H the magnetic field, and c the velocity of light. Since it is only the component of v perpendicular to H that is effective in producing a motional electric field, the high longitudinal velocity imparted to the ion by the space-charge field does not produce Stark quenching. There are two means whereby the ion attains a velocity component in a direction perpendicular to the field:

(1) By thermal and recoil effects. This velocity has been estimated in Sec. IVB to be 1.48×10^5 cm/sec.

(2) By moving under the influence of the crossed transverse space charge field and magnetic field. A value of 0.51×10^5 cm/sec for this velocity has been obtained in Sec. IVF.

The motional field has been calculated at the magnetic field appropriate to the resonance center using a velocity equal to the sum of the above two velocities and the lifetime of the α state found in a field equal to the sum of the maximum space charge field and motional field. The lifetime is $\tau_\alpha=45.2$ μsec. It should be emphasized that the above lifetime is a lower bound to the true lifetime.

D. Collision Quenching

Collisions between metastable helium ions and neutral helium atoms can cause quenching of the former in two ways:

(1) The ion can return to its ground state and its excitation energy pass to an electron of the atom; the electron is ejected with an energy of 16.23 ev.

(2) The ionic charge induces a dipole moment in a neighboring helium atom which remains in its ground state. The ion and atom are in relative motion, with the result that the dipole field sweeps over the ion and transfers it to either the $2\,^2P_{\frac{1}{2}}$ or $2\,^2P_{\frac{3}{2}}$ states, whence there is radiative decay.

The cross sections for these two processes have been estimated by using methods devised by Lamb and Sternberg; at a bombarding current of $\frac{1}{2}$ ma and helium pressure of 4.6 microns, the cross sections and decay

[11] HeI, p. 546, Eq. (23). Note that this latter equation is in error.

[12] N. F. Mott and H. S. W. Massey, *Theory of Atomic Collisions* (Clarendon Press, Oxford, 1949), second edition, p. 236.

times are approximately

$$\sigma_{\text{radiation}}=34.4\pi a_0^2, \quad \tau_r=4.93\ \mu\text{sec},$$
$$\sigma_{\text{ejection}}=15.9\pi a_0^2, \quad \tau_e=10.7\ \mu\text{sec}, \qquad (9)$$
$$\sigma_{\text{total}}=50.3\pi a_0^2, \quad \tau_{\text{total}}=3.37\ \mu\text{sec}.$$

The values of τ_{total} are not strongly dependent upon the bombarding current. However, when the pressure is reduced to 1.3 microns, τ_{total} is increased to 15 μsec due to the change in velocity with space-charge field, and collision quenching no longer is a significant removal process.

E. Electron Quenching

Metastable ions can be quenched in a way similar to that described in Sec. IVD by the passage of an electron past the ion. The cross section has been estimated approximately, by using a method analogous to that from which the pressure-quenching cross sections were obtained. The cross section for 30-volt electrons is approximately $150\pi a_0^2$. However, both the primary and secondary electron flux is so low that negligible quenching results.

F. Space-Charge Effects

Prior to the admission of helium gas the electron beam, as it crosses the cavity, produces a potential well whose depth is 0.75 volt (beam current 0.5 ma). When gas is admitted, ions are produced uniformly along the beam. Since the mean translational energy of an ion, due to thermal and recoil effects, is only about 0.02 electron volt, all ions produced within the cavity are initially trapped there; thus the potential depression is neutralized and a positive ionic space charge builds up until conditions are such that ions are removed from the cavity at the same rate as they are formed. Under the present experimental conditions, volume loss processes are negligible. The mean velocity of the secondary electrons is high, about 3.6×10^8 cm/sec; the equivalent energy is 36.8 ev. Thus the major fraction of the secondaries leave the cavity rapidly and

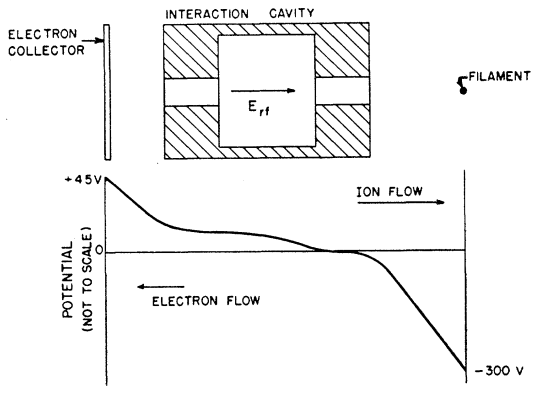

FIG. 7. Approximate potential variation between electron collector and filament.

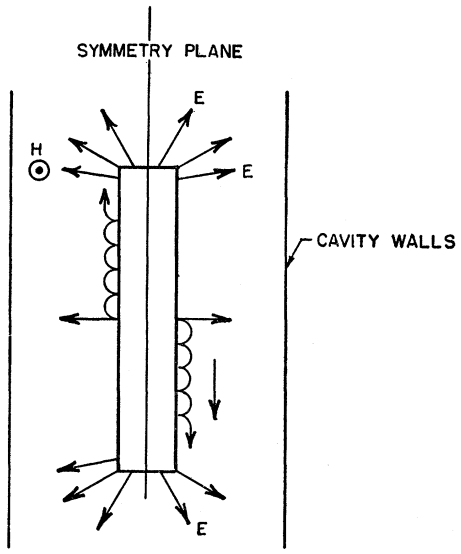

FIG. 8. Transverse space charge field and resulting ion motion.

make only a small contribution to the resultant charge density of ions and electrons, and the possibility that a neutral plasma exists within the cavity can be excluded. Since the collector is held at a positive potential and the filament at a negative potential with respect to the cavity, ions can leave the cavity only at the filament end and electrons at the collector end. As a neutral cloud can be excluded as a possibility, the potential distribution between collector and filament must have the form shown in Fig. 7 and it can be seen that the potential distribution required to remove ions to the right is such as to remove any slow secondaries to the left, a fact which additionally helps reduce any tendency towards neutralization.

An approximate solution for the electric fields inside the cavity has been obtained using a method devised by Helm, Spangenberg, and Field.[13] A brief summary of their results is contained in Appendix II where it is shown that under normal conditions of current and pressure (bombarding current=$\frac{1}{2}$ ma; pressure=4.6 microns) the average removal time for ions produced within the cavity is 1.12 μsec. When the bombarding current is raised to 2 ma, the removal time becomes 0.72 μsec. Ions produced between the electron collector plate and exit slot, in the main enter the cavity with high velocity. If the mean energy of these ions is taken to be 22.5 ev, the appropriate transit time is 0.18 μsec.

The charge cloud extending across the cavity gives rise to an electric field perpendicular to the applied magnetic field, Fig. 8. The cloud is symmetrically situated with respect to the walls of the cavity so that if the whole cloud is assumed to be of uniform density and of infinite extent in two directions, the electric

[13] Helm, Spangenberg, and Field, Elect. Commun. **24**, n. 1, March (1947). A convenient summary is contained in an article by M. E. Hines *et al.* [J. Appl. Phys. **26**, 1157 (1955)].

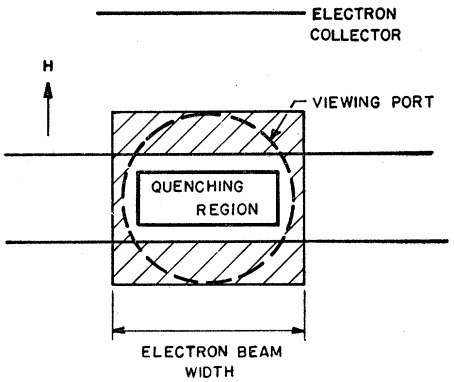

FIG. 9. Cross section of interaction space and viewing port, showing rf quenching region.

field is zero along the plane of symmetry and rises linearly to a maximum value of 8 v/cm (Sec. VIIC) at the edge under normal conditions of current and pressure.

The crossed electric and magnetic fields cause ions to move in cycloidal orbits perpendicularly to both fields with an average velocity $v=cE_s/H$. With $E_s=8$ volts/cm and a magnetic field corresponding to the resonance center $v=0.51\times10^5$ cm/sec. Apart from a small longitudinal field required to remove ions from the cavity, ions on the symmetry plane of the cloud experience zero electric field. However, the transverse field increases linearly as one proceeds to the cloud surface so the cloud would seem to shear itself. But the transverse field changes direction at the edge in such a way that ions tend to be returned to the cloud; ions therefore are not lost to the beam by their transverse motion, but only by their longitudinal motion. In Fig. 9 a cross section of the interaction region is shown. The rf-induced signal comes in the main from the central area denoted "quenching region."

The width of the beam relative to the width of the quenching region depends upon the temperature distribution in the filament. This distribution is in fact not known, although precautions were taken to insure its symmetry with respect to the quenching regions. Therefore it is necessary to consider two cases: (1) The beam is entirely within the quenching region. In this case the signal is unaffected by the transverse motion. (2) The beam extends well beyond the edge of the quenching region. In this case it is necessary to take into account the fact that the actual total transverse motion is small compared to the beam width. The total ion density is unaffected by the transverse motion but both the total number of ions exposed and the exposure time of some of the ions is affected. This effect causes a small resonance shift.

V. LINE SHAPE

If all the metastable ions were exposed to the rf field for the same time t, then aside from certain corrections, the shape of the resulting rf quenching function would be given by

$$\phi(\mu)=N_0(1-e^{-\mu t}), \tag{10}$$

where N_0 is proportional to the rate of production of ions and

$$\mu=\frac{2\pi S_0}{\hbar\omega}\left(\frac{e^2}{\hbar c}\right)\cdot\left(\frac{\gamma\omega}{(\omega-\omega_0)^2+(\gamma/2)^2}\right)|\mathbf{r}\cdot\hat{e}|^2. \tag{11}$$

Here $1/\gamma$ is the mean life of the P state, ω_0 the resonant frequency and ω the frequency of the rf, both in radians/sec. S_0 is the incident power in ergs/cm sec, $\mathbf{r}$ is a vector whose components are the matrix elements of r for the transition, and $\hat{e}$ is a unit vector along the direction of rf polarization.

In fact, the time that an ion spends in the rf field depends upon its position at formation and upon the potential distribution along the beam. A theory of the line shape would require detailed knowledge of this potential distribution. In principle this information is provided by the calculation in Appendix II. However, the theory employed there is at best only semiquantitative and is only intended to provide an order of magnitude estimate of the space charge fields for the purpose of estimating certain corrections. Much of the information that could be provided by a line shape theory is provided by the experimental quenching curves shown in Fig. 10. These curves show the dependence of the normalized rf signal on rf power at two values of the magnetic field. The agreement of the data at the two fields is indicative of the fact that the ion removal processes are not strongly field dependent and that there are no large asymmetries in the resonance curve. Unfortunately the precision with which this is established is not sufficient for the present purposes and it is necessary to rely in part, on an experimental search for a dependence of the apparent value of the shift (S) on experimental parameters.

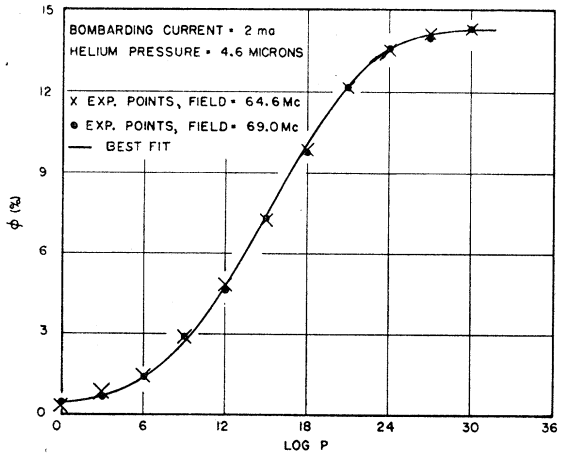

FIG. 10. Quenching curve. Bombarding current=2 ma. Helium pressure=4.6 microns.

VI. PRECISION RESONANCE DATA

Precision resonance data are obtained and treated by a method similar to that described in HeII, Sec. F.

At the start of a run, the power level is adjusted so that the value of ψ at the resonance peak is approximately 30%. A set of five one-minute observations is then made at the working-point fields. Each observation consists of a count taken at low rf power followed by a count taken at high rf power. Three observations are then made at each slope point, the resonance being traversed in a zig-zag fashion to reduce instrumental drifts, and finally the observations at the working points are repeated. At frequent intervals, to check the counting system, a count is taken with the rf power set equal to zero.

Though the total counting time is only about $1\frac{1}{2}$ hours, because of the time required to effect a field change and the large number of instrumental checks that are made, a run lasts about eight hours.

The theory of the Zeeman effect as given by Lamb[14] is used to determine the value of the radiative shift (S) from the observed value of the resonance center field H_0 and the frequency of the rf source. The physical constants entering into the theory of the Zeeman effect are listed in HeII, Sec. F.§

If f_k is the frequency of the rf source, $f\alpha e$ the transition frequency appropriate to the field H_0 as calculated for an assumed value of the radiative shift S_0, then

$$S=f_k-(f_{\alpha e}-S_0). \tag{12}$$

VII. CORRECTIONS AND UNCERTAINTIES

In addition to the uncertainties that arise from purely statistical fluctuations in the observed signal and instrumental parameters, there are a number of effects which influence the final result and contribute slightly to its uncertainty. Table I summarizes these corrections and uncertainties.

TABLE I. Corrections and uncertainties in Mc/sec.

Matrix element variation	
working point fields: 65.0 and 68.6 Mc/sec	-4.34 ± 0.10
working point fields: 64.6 and 69.0 Mc/sec	-4.86 ± 0.10
Zeeman curvature	
working point fields: 65.0 and 68.6 Mc/sec	-0.39
working point fields: 64.6 and 69.0 Mc/sec	-0.58
Stark effect	$+0.04\pm0.02$
Overlap	-0.02 ± 0.01
Field dependence of grid transmission	$+0.03$
Field dependence of space-charge removal	$+0.25\pm0.45$
Magnetic field inhomogeneity uncertainty	±0.40
Uncertainty in scaler dead time correction	±0.30
Uncertainty in Zeeman constants	±0.20

[14] HIII, p. 265.

§ Modification of these constants to account for the differences between the 1952 and 1955 atomic constants and the new theoretical value of the magnetic moment of the electron produces less than a 0.2 Mc/sec change in the present result. See C. M. Sommerfield [Phys. Rev. **107**, 328 (1957)].

A. Matrix Element Variation

Since the matrix element governing the transition depends upon the magnetic field, a significant change in the rf-induced signal between the two working points is introduced, which requires correction. A discussion of this correction and the way it is made may be found in HeII.

B. Zeeman Curvature Correction

The relationship between transition frequency and magnetic field is not quite linear (HIII, Sec. 55). However, in the data reduction a linear relationship has been assumed; the resonance-center field H_0 has been taken to be equal to the average of the corrected working point fields where equal signals obtain. The correction to be applied is the difference between the mean of the transition frequencies at the working-point fields and the transition frequency as obtained from H_0.

C. Stark Effect

The presence of an electric field in the rf interaction region gives rise to a displacement of the fine structure energy levels. The Stark shift of an energy level is easily found by second-order perturbation theory. The requisite matrix elements can be obtained from Table VI of HIII with appropriate modification for the change of nuclear charge Z.

In the present instance there are two known static electric perturbations, (1) the motional electric field, and (2) the field E_s arising from the beam space charge. Since both fields are known only approximately, it suffices to calculate the first at the magnetic field pertaining to the resonance center. For an ion speed perpendicular to H of 1.48×10^5 cm/sec, $E_{\text{motional}}=23.2$ volts/cm. The space charge fields E_s can be estimated from Appendix II. The E_s differ somewhat depending upon the conditions of bombarding current and pressure, but for a current of $\frac{1}{2}$ ma and pressure of 4.6 microns, $E_s=8$ volts/cm, at the outer edge of the charge cloud. Since the field varies linearly from the center to the edge of the charge cloud, the Stark shift has been calculated in a field equal to the sum of the motional field and half the value of the space-charge field at the edge of the cloud, i.e., in a field

$$E=E_{\text{mot}}+E_s/2. \tag{13}$$

Since the resultant field is mainly transverse to H, the level α couples with level f but not e, and e couples only with β. There are, of course, couplings to some sublevels of the $2\,^2P_{\frac{3}{2}}$ state, but because of the large fine-structure separation their effect upon the Stark shift can be neglected. The small longitudinal space-charge field that must be present to drive ions from the cavity does couple α with e but again the effect is negligible.

Both the α and e levels are raised in energy by the electric perturbation, but e more than α because of the

smaller separation between e and β. Thus the value of the transition frequency for αe is lowered, implying a positive correction to S. Under normal conditions of pressure and current,

$\Delta\alpha = 0.02$ Mc/sec, $\Delta e = 0.06$ Mc/sec, $\Delta S = 0.04$ Mc/sec.

These corrections are uncertain insofar as they depend upon the transverse ion velocity and space-charge density. Since the main contribution to the Stark shift arises from the motional rather than the space-charge electric field, the uncertainty in the correction is due principally to the uncertainty in the transverse velocity. If the latter uncertainty is assumed to be 20%, the shift ΔS is 0.04 ± 0.02 Mc/sec. In view of the fact that little or no evidence exists of signal instability due to wall charging, no Stark shift has been assigned as attributable to this cause.

In addition to the dc electric field, the ions are acted upon by the fluctuating Holtsmark[15] field of the space charge cloud. At the ion densities present in the beam the Holtsmark field is about one hundred times less than the dc electric field and produces a negligible Stark shift. Likewise, the small rf Stark shift discussed in HIII, Appendix IV, is quite negligible.

D. Overlap Corrections

In addition to the desired transition αe, the rf field may stimulate the transitions βf and αf and overlapping of these latter resonances with αe may introduce a distortion. The transition βf is, like αe, a π transition and might generally be expected at high rf power to overlap significantly with αe. However, the radio frequency has been chosen so that the center of the αe resonance lies very close to the βf crossing point. Thus the overlap of αe by βf is symmetrical because of the choice of frequency, and small because of the large separation in field between the two resonance centers, and no significant shift in the αe resonance center is produced. If the geometry of the cavity were perfect and if the cavity were perfectly aligned with the magnetic field the σ transitions αf and βe would not be excited. In actual fact, the distortion of the cavity by the beam apertures introduces a small transverse component of rf electric field. A detailed estimate of the field distortion indicates that the effective value of the transverse rf field component is about 1/50 of the desired parallel component. Considerable care was taken in the design of the apparatus to ensure that the rf electric field lay parallel to the magnetic field lines. The two fields should not be more than a fraction of a degree out of parallel, but to set an upper bound to the effect an angle of two degrees was used in estimating the overlap shift. The magnitude of the overlap correction depends on the β-state population. If the α- and β-state population were equal the correction would be -0.03 Mc/sec. If the β-state population were zero, the correction would be -0.001 Mc/sec. In point of fact, the β-state population is not known. Since the experiment was performed at the βf crossing point the Stark quenching of the β state in certainly more rapid than that of the α state. However, the best estimates indicate a β-state Stark lifetime of 2.7 μsec. Since this time is considerably longer than the time necessary for an ion to drift across the cavity it is likely that the α- and β-state populations are nearly equal. In view of the uncertainty in the β-state population, the overlap correction is taken as -0.02 ± 0.01 Mc/sec.

[15] Kivel, Bloom, and Margenau, Phys. Rev. 98, 495 (1955).

E. Pressure Quenching

The major fraction of the experimental runs was made at a helium pressure of 4.6 microns. At this pressure, quenching of metastable atoms by collision with neutral gas atoms is a significant removal process (see Sec. IVD) and it is of importance to examine the magnetic field dependence of the collision cross sections to determine if an appreciable distortion of the resonance could result. Since the cross section for radiative pressure quenching is the largest, a calculation has been made with first-order perturbation theory of this cross section at the two working points, which takes into account the change in the energy levels with magnetic field. The cross section calculated is within 10% of that obtained from the exact calculation of Lamb at zero field and changes by only one part in 10^5 between the two working points. The resonance shift produced by the change of cross section is negligible. However, the possibility exists that during an elastic collision the perturbation of the $2S-2P$ level system may be sufficient to produce a shift in the resonance center. The perturbing field is produced by the induced dipole moment in a neighboring neutral atom. The best available estimate of this effect indicates that the resulting shift is negligible.

F. Grid Transmission

The primary electrons have a thermal velocity component perpendicular to the magnetic field and pass through the cavity in tight spirals around the field lines. Since the radius of curvature of these spirals depends upon the magnetic field, the fraction of the incident electrons intercepted by the vanes that divide the beam entrance and exit slots is field dependent and a larger fraction of the incident current passes through the cavity as the magnetic field is increased. However, during a run it is the current to the collector that is held constant and as a consequence, the electron density within the cavity is higher at the low-field working point than at the high. There is thus a small increase in R, the rate of production of ions, which produces a change in the equilibrium ion density and ion removal time. The change in equilibrium ion density is small amounting to about two parts in 10^4 and the resulting correction to S is $+0.03$ Mc/sec.

G. Field Dependence of Space Charge Removal

It has been estimated that the transverse space charge motion discussed in Sec. IVF produces a shift of about $+0.35\pm0.35$ Mc/sec. In addition there is an estimated shift of -0.1 ± 0.1 Mc/sec resulting from a change in the width of the ion cloud as the magnetic field is varied. There are other possible field dependent space charge effects which may give rise to shifts. It has not been possible to make reliable estimates of these effects and it is therefore necessary to rely on the observed values of the resonance center under different space charge conditions to establish that the resulting shifts are not large.

H. Magnetic Field Inhomogeneity

The magnetic field inhomogeneity correction (Sec. IID) was measured once during the course of the experiment. The uncertainty due to this measurement (±0.4 Mc/sec) is thus contributed in its entirety to the final value of S.

VIII. RESULTS AND DISCUSSION

In all, 38 runs were made, 26 of which have yielded successful determinations of S. Instrumental and other difficulties led to the rejection of the remainder.

The runs fall into five groups. Four groups contain runs taken under differing conditions of bombarding current or helium pressure to determine whether space-charge conditions within the beam are influential upon S; the remaining group is the result of an attempt to determine the presence of a resonance asymmetry. The results are contained in Table II.

The values of S in Column A are the weighted means of the several runs that comprise a group, corrected only for field inhomogeneity, matrix element variation and Zeeman curvature. The weighting factors are, with the exception of runs 7, 21, 22, and 27, taken to be proportional to the reciprocal squares of the uncertainties in S based on the theoretical counting statistics and the estimated instrumental fluctuations; in the exceptional cases the observed counting fluctuation is used in place of the theoretical fluctuation (see Section IIID). Except for Group 1, the uncertainties quoted in A are the observed standard deviations. In Group 1 the observed

TABLE II. Summary of results.[a]

Group	A S(Mc/sec) (Partially corrected)	B S(Mc/sec) (Fully corrected)	Number of runs	Bombarding current (ma)	Pressure (microns)
1	14 039.0±1.4	14 039.3±2.8	5	0.5	4.6
2	14 041.9±1.8	14 042.2±3.2	5	0.5	4.6
3	14 037.9±2.5	14 038.2±3.9	5	0.1	4.6
4	14 038.1±2.4	14 038.4±3.8	6	2.0	4.6
5	14 044.1±2.9	14 044.4±4.3	5	0.5	1.3

[a] The runs comprising Group 1 were taken at working point fields of 65.0 and 68.6 Mc/sec in terms of the proton resonance frequency. All others were taken at 64.6 and 69.0 Mc/sec.

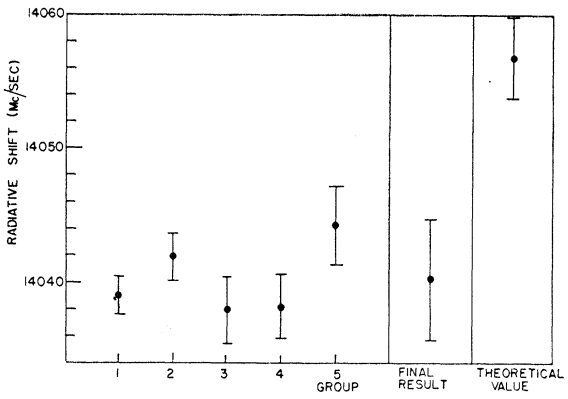

FIG. 11. Graphic representation of the partially corrected results and their statistical uncertainties (Table II, column A).

standard deviation is about half of that expected from the uncertainty in each of the several runs that constitute the group. In this case the expected uncertainty is used in place of the observed standard deviation. The results with all of the corrections applied are listed in column B. Here the uncertainties in the corrections have been simply added to the uncertainties quoted in column A. For the purpose of disclosing resonance shifts the results of column A together with their statistical uncertainties are shown in Fig. 11. It can be seen that within the present statistical uncertainty there is no experimental evidence for either a current- or pressure-induced shift or a resonance asymmetry. The final result is obtained by combining the fully corrected results (Column B of Table II) into a grand weighted mean with weighing factors obtained from the statistical uncertainties listed in column A of Table II. The standard deviation of this mean is 1.0 Mc/sec. In view of the uncertainties in the space charge corrections and accordance with the previous practice in the hydrogen experiments, we adopt as a measure of the overall reliability of the final results a "limit of error." This is taken as three times the standard deviation (3.0 Mc/sec) plus the estimated uncertainty in the corrections (1.5 Mc/sec). The final result is

$$S=14\,040.2\pm4.5 \text{ Mc/sec}$$

This result is in good agreement with the value of S determined by Novick ($14\,043\pm13$ Mc/sec) and Skinner ($14\,020\pm100$ Mc/sec).

Using the value of the fourth order magnetic moment of the electron as recently computed by Sommerfield, the theoretical value for the radiative shift in singly ionized helium is,[16] for a point nucleus, $S_p=14\,048.8\pm2.1$ Mc/sec. A correction must be added due to the finite nuclear size. Using a recent value for the α particle

[16] C. M. Sommerfield, Phys. Rev. **107**, 328 (1957). Dr. Sommerfield has kindly informed us that his value for the shift in helium ($14\,055.9\pm2.1$ Mc/sec) includes a finite size correction of $+7.1$ Mc/sec. This correction is based on an early value of the α-particle radius. [See Novick, Lipworth, and Yergin, Phys. Rev. **100**, 1153 (1955)].

radius,[17] the correction is $+8.0\pm0.9$ Mc/sec. The large uncertainty in the correction arises from the uncertainty in the determination of the radius. For a finite nucleus then $S_{\text{theor}}=14\,056.8\pm3.0$ Mc/sec. This value differs significantly from the present experimental result.

If we let $\delta(Z)$ be the difference between the experimental and theoretical values of the Lamb shift in an atom of nuclear charge (Z), then for hydrogen[16] $\delta(1)=-0.22\pm0.23$ Mc/sec and for helium $\delta(2)=-16.6\pm7.5$ Mc/sec. In each case the uncertainty assigned to δ is the sum of the theoretical and experimental uncertainties. The question now arises as to whether the large discrepancy in helium can be reconciled with the almost negligible discrepancy in hydrogen. A similar question was discussed at the conclusion of HeII, using the hypothesis, based on quantum electrodynamical considerations, that the (Z) dependence of δ should to a sufficient accuracy for the present purposes, be expressible as a linear combination of terms of the form Z^4, Z^5, and $Z^6\ln(\alpha Z)$. At that time the hydrogen discrepancy was $\delta(1)=+0.65\pm0.26$ Mc/sec and the helium discrepancy was $\delta(2)=0\pm16.0$ Mc/sec and it was concluded that these values could not be reconciled by a single term of order $Z^6\ln(\alpha Z)$ though they could be reconciled by a single term of order Z^4 or Z^5 having a coefficient of at least $+0.39$ Mc/sec. At that time it appeared most unlikely that the theory would yield such a large coefficient for Z^4 or Z^5 terms. Recently Sommerfield[16] has shown that a revised estimate of the fourth order magnetic moment of the electron yields a correction to the previous calculation of the form $+0.836Z^4$ Mc/sec. It is principally this correction which reduced the hydrogen discrepancy to its present low value. A very attractive hypothesis regarding the present helium discrepancy is that it is due to a single term of order $Z^6\ln(\alpha Z)$. Baranger, Bethe, and Feynman[18] have suggested that a relativistic term of this form exists and that its magnitude for hydrogen might be as large as 0.25 Mc/sec. If this is indeed so and if the sign of the term is negative then it will produce essentially perfect agreement between theory and experiment in both hydrogen and helium since the hydrogen discrepancy will be reduced to -0.03 ± 0.23 Mc/sec and the helium discrepancy to -2.6 ± 7.5 Mc/sec. The magnitude of this relativistic term could be as low as 0.16 Mc/sec for hydrogen and still be in agreement with the helium data. It is clearly desirable that this relativistic term be evaluated as soon as possible. It is also possible to reconcile the hydrogen and helium results with a single negative term of order Z^5. However, the magnitude of the coefficient of such a term must be at least 0.28 Mc/sec.

[17] R. W. McAllister and R. Hofstadter, Phys. Rev. **102**, 851 (1956).

[18] Baranger, Bethe, Feynman, Phys. Rev. **92**, 482 (1953).

ACKNOWLEDGMENTS

The authors wish to thank Professor N. M. Kroll and Professor P. Kusch for their guidance and support, Mr. M. McDermott and Dr. A. G. Prodell for their assistance in the experimental phases of the work, and the staff of the Radiation Laboratory for their wholeheated cooperation, especially C. Dechert, A. W. Costello, L. Karasyk, and L. B. Alsop.

APPENDIX I

The counting rates are such that an appreciable dead-time correction must be applied to observed counts in order to obtain true counts. The dead-time correction required has been shown empirically to be of the "extended" type,[19] where the relation between the observed counting rate $N(o)$ and the true counting rate $N(t)$ is

$$N(o)=N(t)e^{-2N(t)\tau/T}. \tag{14}$$

Here τ is the dead time and T the counting interval; the factor 2 is present since each scaler counts on a 50% duty cycle. The dead time τ is measured by injecting into the input circuit of the first amplifier a signal derived from an RCA. 5819 photomultiplier tube in a light-tight box. A small lamp inside the box serves as

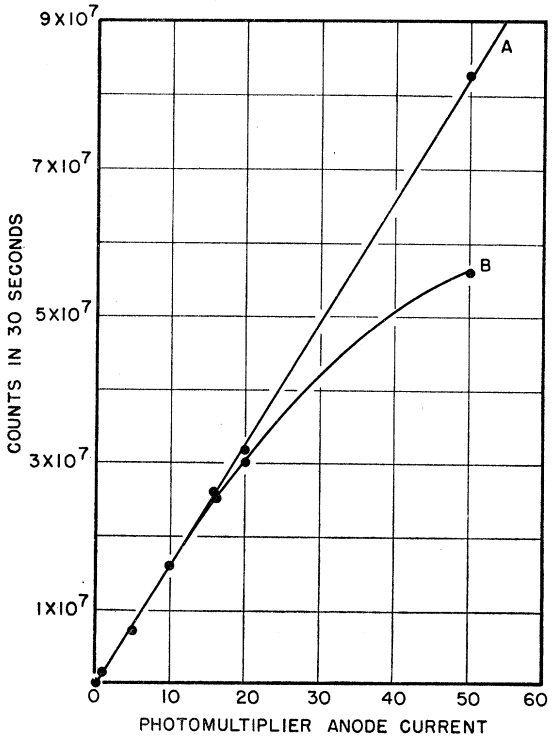

FIG. 12. Curve A: Counts corrected for dead time loss—extended theory. Curve B: Counts corrected for dead time loss—linear theory.

[19] D. Halliday, *Introductory Nuclear Physics* (John Wiley and Sons, Inc., New York, 1950), first edition, p. 209.

a signal source. The 5819 anode current is assumed to be proportional to the true counting rate.

Curve A in Fig. 12 is a plot of photomultiplier anode current *versus* true counting rate as obtained from the above formula. It will be seen that the "extended" dead-time theory accounts excellently for the dead time losses, to counting rates far in excess of those met with in practice.

Curve B is based on the simple linear or nonextended dead-time law

$$N(t)=N(o)\Big/\left(1-\frac{2\tau N(o)}{T}\right),$$

and it is evident that departures occur at counting rates of the order of 10^6/sec.

However, the linear law is still useful at a counting rate below 5×10^5/sec, and since data reduction is appreciably simplified by use of the linear correction, it has been the one almost exclusively employed. During the series of runs taken at high bombarding current, the counting rate was reduced to a value where the linear correction could be applied by increasing the thickness of the Formvar film separating the main and detector regions of the apparatus.

The dead-time τ has been measured before and after the main body of precision runs and is approximately 0.15 μsec. Photomultiplier fatigue and the difficulty of maintaining the strength of the light source constant has limited the measurement of τ to an accuracy of about 10%; fortunately, however, the precise value of τ need not be known as ϕ_H and ϕ_L are determined as the ratio of two approximately equal counts. The effect of the uncertainty in τ upon the final result has been estimated by reducing three runs with τ taken equal to zero. An additional uncertainty of about 0.2 Mc/sec is thereby introduced into the final value of (S).

If the rf power is set equal to zero and the count in Channel I is compared with that in Channel II, it is found that they are not quite equal. A typical value for the ratio $N_{\rm II}/N_{\rm I}$ is 1.0007. Slight differences either in the widths of the two gate pulses or in the times required to switch on the gate circuits (due to differences in circuit constants) could be the cause of this effect. It might also be attributed to small differences in the dead times of the two scalers. The true cause could not be readily ascertained. The ratio $N_{\rm II}/N_{\rm I}$ can be varied by varying the bias voltages on the scaler input tubes. In practice the biases are adjusted until the ratio is as close to unity as possible; the settings once established are stable. During the course of a run several observations with zero rf power are made to obtain a value of the ratio for that run and a correction applied which consists of reducing the $N_{\rm II}$ counts by that ratio prior to obtaining the ϕ_H and ϕ_L. All runs were reduced with and without this correction applied. The change in the value of the radiative shift produced by the inclusion of this correction is about 0.2 Mc/sec, and seems to have no consistent sign; an additional uncertainty of this amount has been included in the final uncertainty.

APPENDIX II

Consider for the moment only those ions produced within the cavity. It is shown in reference 13 that if thermal and recoil velocities and gas collisions are neglected, the ionic charge density $\sigma_i(Z)$ at a point Z within the ion beam is given by the expression

$$\sigma_i(Z)=\frac{R}{(2e\lambda/m)^{\frac{1}{2}}}\int_0^Z\frac{dZ'}{[\sigma_i(Z')-\sigma_i(Z)]^{\frac{1}{2}}},\qquad(15)$$

where R is the rate of production of ions per unit volume by the electron beam, e/m is the charge-to-mass ratio of the ions, and $\lambda=dL/4\epsilon_0$, d being the thickness of the electron beam (assumed equal to the filament diameter because of the presence of a strong magnetic field) and L being the cavity width in a direction perpendicular to the plane of the beam.‖

The solution of the above integral equation is

$$\frac{3\pi RZ}{2[\sigma(0)]^{\frac{3}{2}}(2e\lambda/m)^{\frac{1}{2}}}=\left[1+\frac{2\sigma(Z)}{\sigma(0)}\right]\left[1-\frac{\sigma(Z)}{\sigma(0)}\right]^{\frac{1}{2}}.\qquad(16)$$

A plot of this expression is shown in Fig. 13. The charge density and therefore the potential has infinite slope when $\sigma_i(Z)=\frac{1}{2}\sigma_i(0)$, when the left hand side of (16) is equal to $\sqrt{2}$. If it is assumed that the high gradient of potential due to charge density must join smoothly

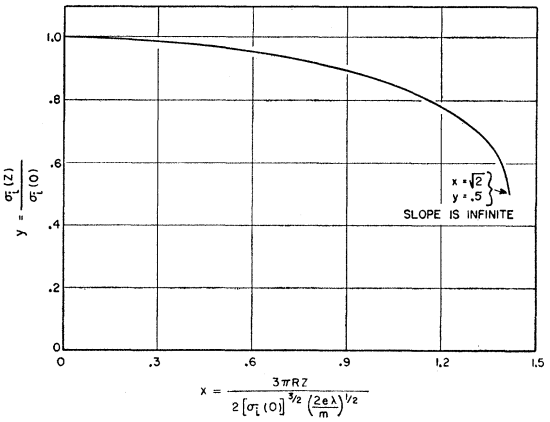

FIG. 13. Theoretical variation of ionic charge density with distance along the beam.

‖ *Note added in proof.*—This theory is based on the assumption that the charges are distributed in a long thin beam and that the potential variation is mostly in the transverse direction. In the present instance the beam is in fact quite short and it may be objected that the theory is not applicable. An approximate calculation has been made which takes account of the finite length of the beam. The electric fields obtained in this calculation are comparable to but somewhat smaller than the fields obtained above. Since the results of the present calculation are only being used as a basis for estimating certain small corrections there is no need to refine the calculation.

TABLE III. Ion and electron densities.

Bombarding current (ma)	Helium pressure (microns)	Electrons electrons/cc	R ions/cc sec	Ions ions/cc
1/10	4.6	0.25×10^{8}	7.34×10^{13}	1.61×10^{8}
1/2	4.6	1.23×10^{8}	3.67×10^{14}	4.71×10^{8}
2	4.6	4.92×10^{8}	1.47×10^{15}	11.9×10^{8}
1/2	1.3	1.23×10^{8}	1.03×10^{14}	2.03×10^{8}

with the high gradient of the electron accelerating potential at the entrance to the cavity, where $Z=h$ (the cavity length), then

$$\frac{3\pi Rh}{2(2e\lambda/m)^{\frac{1}{2}}[\sigma(0)]^{\frac{3}{2}}}=\sqrt{2}. \tag{17}$$

$\sigma(0)$ can be obtained from Eq. (17), $\sigma(Z)$ from Fig. 13. If the charge density is a slowly varying function of position along the beam, it can be shown that the potential within the beam is given by

$$V(Z)=\lambda[\sigma_{\text{ion}}(Z)+\sigma_{\text{electron}}(Z)]. \tag{18}$$

This relation is used in Appendix III, where the theory of the line shape is discussed.

Some relevant ion and electron densities are listed in Table III. The value of R used is based on the value[20] of $\alpha/p=0.648$ for 300-ev electrons; α is the number of ions produced per cm by a single electron and p is the pressure in mm of mercury.

In order to define a mean life for ion removal by the space charge fields, consider the density $\sigma(m)$ at the center of the rf region. Then neglecting for the moment high-speed ions produced in the collector region, we must have by charge conservation

$$SR=\sigma(m)\bar{v}, \tag{19}$$

where R is the rate of production of ions/unit volume of the beam, $2S$ is the total length of the interaction region from entrance to exit slot and $\bar{v}$ is the average velocity of the ions at the center of the cavity. Thus an average removal time τ for ions produced within the cavity is given by

$$\tau=d\sigma(m)/SR, \tag{20}$$

where d is the cavity height. Under normal conditions of current and pressure (bombarding current $=\frac{1}{2}$ ma, pressure$=4.6$ microns),

$$\tau=1.12\ \mu\text{sec}, \tag{21}$$

when the bombarding current is raised to 2 ma,

$$\tau=0.72\ \mu\text{sec}. \tag{22}$$

Ions produced between the electron collector and exit slots in the main enter the cavity with high velocity. If the mean energy of the collector ions is taken to be $22\frac{1}{2}$ volts, the appropriate removal time for the collector ions is 0.18 μsec.

[20] *International Critical Tables* (McGraw-Hill Book Company, Inc., New York, 1929), Vol. 6, p. 120.